MICROFABRICATED NEAR-FIELD MICROWAVE PROBES FOR SCANNING MICROSCOPY

Yaqiang Wang and Massood Tabib-Azar
Department of Electrical Engineering and Computer Science
Case Western Reserve University, Cleveland, OH 44106
Tel.: (216) 368-6431, Fax: (216) 368-6039, email: tabib-azar@cwru.edu

ABSTRACT

The design and microfabrication of a silicon co-axial scanning near-field microwave probe (SNMP) compatible with atomic force microscope (AFM) system are reported. Scanning near-field microwave microscopy (SNMM) imaging is suitable for nondestructive surface and subsurface characterization of materials over a wide frequency range-between 0.1 GHz and 300 GHz, which bridges the frequency gap among other scanning local probe microscopy (SLPM) methods. The microfabricated SNMP consists of a silicon (Si) V-shaped cantilever beam, a co-axial tip, and aluminum waveguides. The design and microfabrication procedure are described. Mechanical and electrical characterizations, and simultaneous contact AFM and SNMM surface imaging are presented.

INTRODUCTION

Scanning local probe microscopy (SLPM) has enabled us to image atoms [1], electrons' conduction path in solids [2], and their spins [3]. Local scanning probes such as scanning tunneling microscope (STM), AFM, magnetic force microscope (MFM), scanning capacitance microscope (SCM), and near-field scanning optical microscope (NSOM) have become important tools in imaging of materials with 1Å-500 nm resolutions. However, among the DC and low frequency measurements (≤ 1 GHz) offered by STM, AFM, MFM, SCM on the left hand and optical frequency offered by NSOM on the right hand, there is a very large frequency gap (figure 1) that is not covered by existing SLPM tools. SNMM offers the possibility of imaging with signals from 0.1 GHz up to 300 GHz, bridging the frequency gap in SLPM tools. Its significance also lies in the ability to nondestructively characterizing surfaces and sub-surfaces of materials [4-6].

The heart of SNMM is an AFM-compatible SNMP that was designed, fabricated, and characterized as discussed in the following sections.

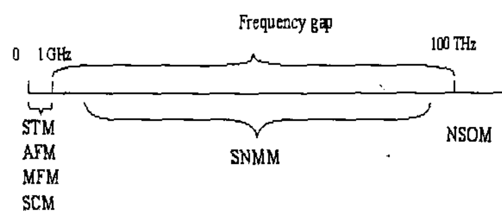

Figure 1. Frequency spectrum for different SLPM tools.

SNMP DESIGN

The proposed SNMPs are comparable with commercial AFM probes in dimension as well as mechanical characteristics and optical reflectance. The probe has two parts. First, V-shaped cantilever beam of the probes operate with resonant frequencies 10-200 KHz and the spring constants 0.1-10 N/m. It is well known that the spring constant K for V-shaped cantilever beam is

$$K = \frac{6EI}{L^3} = \frac{EW}{2}\left(\frac{t}{L}\right)^3 \tag{1}$$

The resonant frequency f_0 is expressed by

$$f_0 = \frac{3.52}{\pi}\frac{t}{L^2}\sqrt{\frac{E}{12\rho}} \tag{2}$$

where W is beam width, L is the beam length, and t is the beam thickness. Silicon Young's modulus is E=130 GPa, density ρ=2330 kg/m^3, the beam width was designed to be 50 µm, its thickness 3-5 µm, and its length 300 µm-1000 µm.

The second part of the probe is the tip section integrated with the cantilever beam. The tips were formed by SF_6 plasma etching followed by low temperature oxidation sharpening [7]. Each probe chip size was 3.6 mm

)-7803-7731-1/03/$17.00 ©2003 IEEE

long and 1.6 mm wide, compatible with commercial AFM probes.

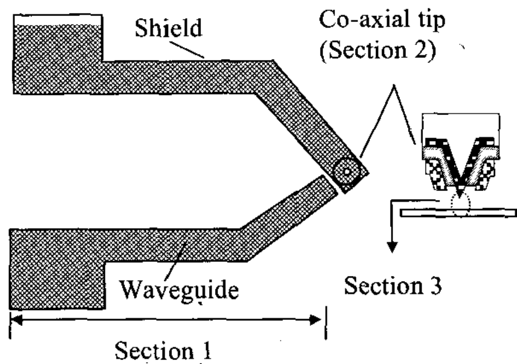

Figure 2. Electrical parts of the SNMP.

From the microwave point of view, the probe had three main sections, as shown in Figure 2. The first section was the waveguide that guided the microwave signal from the generator to the probe tip. The second section was the tip region that confined the fields by its conical shape and coaxial geometry. The third section was the tip-sample interaction section. The electrical models for each section were analyzed elsewhere [8].

MICROFABRICATION AND RESULTS

The starting substrate was a 4-inch double-side polished silicon on insulator (SOI) wafer with device layer 15 μm, buried oxide layer 1 μm, and handle layer 400 μm. Both silicon device layer and handle layer were p-type with (100) orientation. Over 300 probe chips can be batch fabricated per wafer. The main steps were illustrated in Figure 3. The cross-section view was along the AA' line direction.

After a RCA clean, the SOI wafer was thermally oxidized at temperature of 1200 °C to grow 1 μm SiO_2. The photolithography step No.1 defined circular patterns for silicon tip etching. Then the exposed thermal oxide was etched away by Buffered HF (BHF). After that, SF_6 plasma etching was performed to realize conical silicon tips. Sharp silicon tips were achieved with a low temperature thermal oxidation sharpening at 950 °C (figure 3a). Next, the photolithography step No.2 exposed the tip region that was made conductive by a boron ion implantation. The ion implantation was performed with a dose of 5E16 ions/cm^2 at 60 Kev (figure 3b).

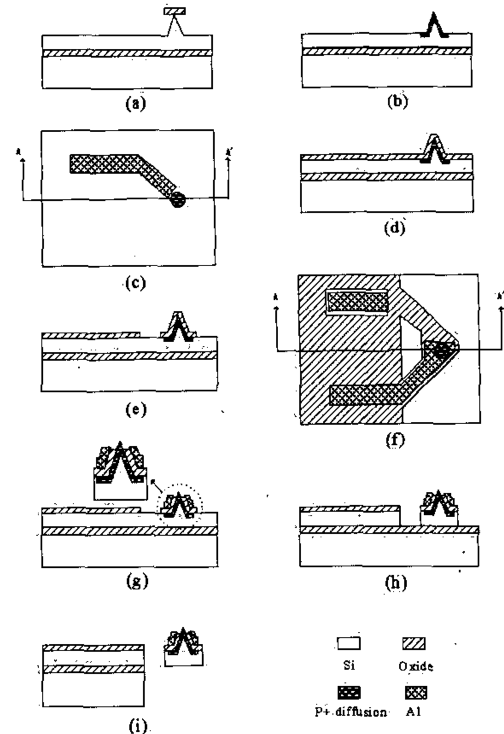

Figure 3. Microfabrication process flow.

A 5000 Å aluminum (Al) was sputtered at the pressure of 1E-7 Torr. The Al waveguide was defined by the photolithography step No.3 and patterned by wet etch (figure 3c). LPCVD was followed to deposit a 3000 Å Low Temperature Oxide (LTO) at 450 °C in the furnace at the pressure of 350 mTorr (figure 3d). Another layer of 1 μm Al was sputtered and patterned by the photolithography step No.4 to form a metal shield layer. The 3000 Å LTO layer acted as an isolation layer between the waveguide and the shield layer at the tip region. The photolithography step No.5 was used to pattern the LTO layer after metal wet etch to expose the underneath Al waveguide (figure 3e and figure 3f).

A special processing technique named "tip exposure" was implemented to realize the co-axially shielded tip structure that confined the electromagnetic field in the exposed tip region during microwave measurements. First, a thick photoresist AZ® 9260 was spun to achieve uniform coating on the wafer. Then a plasma system M4L was utilized to etch the photoresist to expose the Al-coated tip. The aperture in the shield layer was formed by an Al wet etching.

The conductive silicon tip was exposed by the following LTO etch to achieve the co-axial structure (figure 3g). Silicon anisotropic plasma etching was done after the photolithography step No.6 to define a V-shaped cantilever beam with thickness 3-5 μm (figure 3h). AZ® 9260 was spun again to protect the device layer before the backside of the handle layer underwent the last

photolithography step. Double-sided alignment was used to define the backside DRIE region to form the V-shaped cantilever beam. After DRIE, the SNMP was released by an oxide-etching step followed by photoresist stripping (figure 3i).

Figure 4 includes two SEM photos of silicon tips after plasma etching and oxidation sharpening. The apex curvature was around 10 nm. Figure 5 is the SEM photo of a co-axial tip. Figure 6 is the SEM photo of a released SNMP.

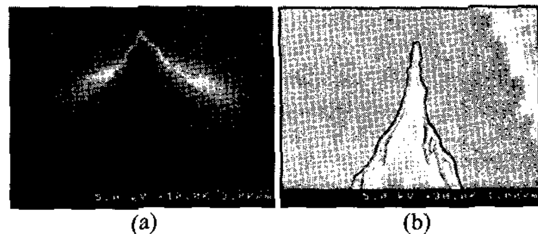

(a) (b)

Figure 4. **(a)** SEM photo of a silicon tip. **(b)** SEM photo of a tip apex region after oxidation sharpening.

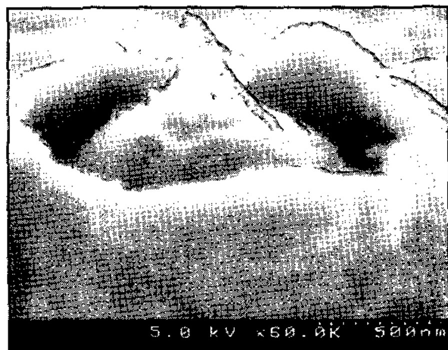

Figure 5. SEM photo of a co-axial tip.

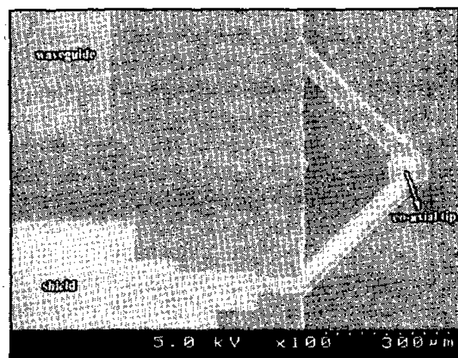

Figure 6. SEM photo of a microfabricated SNMP.

SNMP CHARACTERIZATION

A commercially available ThermoMicroscopes Explorer^{TM} AFM system was used to measure the microfabricated SNMPs' mechanical properties. Figure 7 shows an oscillation spectrum of an SNMP with L=300 μm, W=50 μm, and t = 5μm. The measured resonant frequency was 170.92 KHz, and calculated Q factor in air was 317.

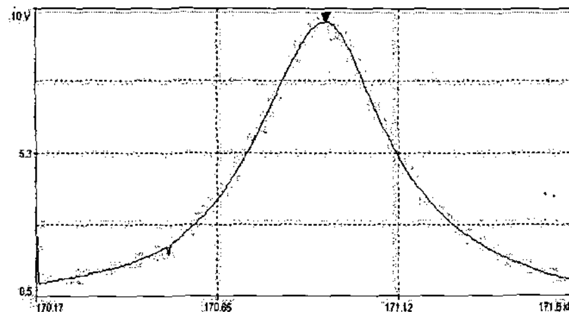

Figure 7. Mechanical oscillation spectrum.

The electrical characterization was performed by using a HP 8720C network analyzer to measure the input reflection coefficient magnitude $|S_{11}|$ with and without a sample presence. Figure 8 shows the $|S_{11}|$ spectra of an SNMP tip in air and over a metallic sample from 50 MHz to 20 GHz. The top curve in figure 8 shows ($|S_{11}|$ + 50) dB in air. The middle curve is the values of ($|S_{11}|$ + 25 dB) measured when approaching the microwave probe to a metal sample in the same frequency range. After subtracting the $|S_{11}|$ values in air from the $|S_{11}|$ values over the sample, the bottom curve of figure 8 was obtained. This curve shows sensitive frequencies for microwave microscopy applications. For example, it can be seen that there are peaks around 1 GHz, 3 GHz, and 5 GHz. This indicates that microwave scans at these frequencies would yield large variations where the sample's microwave properties change.

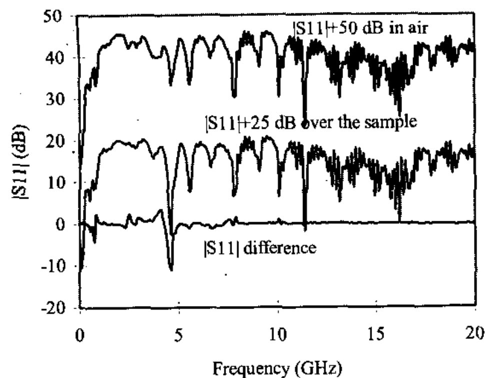

Figure 8. Reflection ($|S_{11}|$) spectra of tip in air and over a metallic sample.

APPLICATION

We have implemented the microfabricated SNMPs for SNMM applications using Explorer^{TM} AFM systems. Simultaneous contact mode topography and SNMM images on a grid sample are shown in Figures 9 and 10.

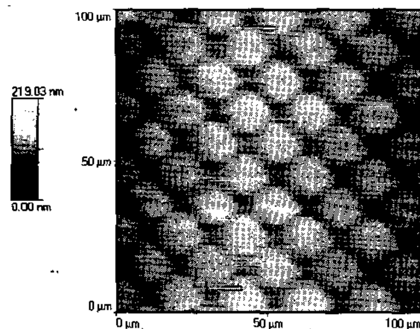

Figure 9. Contact AFM image.

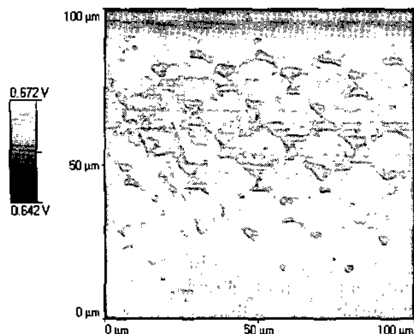

Figure 10. SNMM image with an SNMP simultaneously performed with the contact AFM measurement.

SUMMARY AND OUTLOOK

We have demonstrated the microfabrication of AFM compatible SNMPs with integrated co-axial tips. First simultaneous contact AFM and SNMM surface images were reported. Currently, we are fabricating new generation SNMPs. In future work, we will apply the SNMPs for more scanning microscopy applications, such as imaging biological objects as well as electronic devices and structural materials.

Acknowledgments

We would like to thank Mr. T. Zhang for the SNMM surface imaging. This work was supported by NIST. The probes were fabricated in the Microfabrication Laboratory at Case Western Reserve University.

References

1. Gregory A. Fiete, Jesse S. Hersch, Eric J. Heller, H. C. Manoharan, C. P. Lutz, and D. M. Eigler, "Scattering Theory of Kondo Mirages and Observation of Single Kondo Atom Phase Shift," *Phys. Rev. Lett.*, **86**, pp. 2392-2395 (2001).
2. I. H. Chan, R. M. Westervelt, K. D. Maranowski, and A. C. Gossard, "Strongly capacitively coupled quantum dots," *Appl. Phys. Lett.*, **80**, pp. 1818-1820 (2002).
3. A. Kubetzka, M. Bode, O. Pietzsch, and R. Wiesendanger, "Spin-Polarized Scanning Tunneling Microscopy with Antiferromagnetic Probe Tips," *Phys. Rev. Lett.*, **88**, 057201 (2002).
4. Björn T. Rosner and Daniel W. van der Weide, "High-frequency near-field microscopy," *Rev. Sci. Instrum.*, **73**, pp. 2505-2525 (2002).
5. Yaqiang Wang and Massood Tabib-Azar, "Microfabricated Near-field Scanning Microwave Probes," *IEEE Electron Devices Meeting, IEDM '02.*, pp. 905-908 (2002).
6. M. Tabib-Azar, P. S. Pathak, G. Ponchak, S. R. LeClair, "Nondestructive Superresolution Imaging of Defects and Nonuniformities in Metals, Semiconductors, Dielectrics, Composites, and Plants Using Evanescent Microwaves." *Rev. Sci. Instrum.*, **70**, pp. 2783-2792 (1999).
7. T. S. Ravi, B. Marcus, and D. Liu, "Oxidation sharpening of silicon tips," *J. Vac. Sci. Technol. B*, **9**, pp. 2733-2737 (1991).
8. M. Tabib-Azar, D. Akinwande, G. Ponchak, S. R. LeClair, "Novel Physical Sensors Using Evanescent Microwave Probes," *Rev. Sci. Instrum.*, **70**, pp. 3381-3386 (1999).